Chemical Engineering Science 184 (2018) 52–61

Contents lists available at ScienceDirect

Chemical Engineering Science

journal homepage: www.elsevier.com/locate/ces

Cubic equations of state extended to confined fluids: New mixing rules and extension to spherical pores

Gabriel D. Barbosa [a], Michelle L. D'Lima [b], Shaden M.H. Daghash [b], Marcelo Castier [b], Frederico W. Tavares [a,c], Leonardo Travalloni [a,*]

[a] Escola de Química, Universidade Federal do Rio de Janeiro, C.P. 68542, Rio de Janeiro, Brazil
[b] Chemical Engineering Program, Texas A&M University at Qatar, P.O. Box 23874, Doha, Qatar
[c] Programa de Engenharia Química – COPPE, Universidade Federal do Rio de Janeiro, C.P. 68542, Rio de Janeiro, Brazil

HIGHLIGHTS

- A Peng-Robinson-based model of confined fluid mixtures was modified.
- More explicit and consistent mixing rules were adopted.
- An improved performance in mixture adsorption predictions was obtained.
- The adopted pore geometry can affect significantly the model performance.

ARTICLE INFO

Article history:
Received 5 December 2017
Received in revised form 2 March 2018
Accepted 24 March 2018
Available online 27 March 2018

Keywords:
Equation of state
Peng-Robinson
Confined fluids
Porous media
Adsorption

ABSTRACT

The thermodynamic behavior of fluids confined in nanopores is highly influenced by the interaction between fluid molecules and pore walls. The most accurate approaches for modeling confined fluids are too computationally demanding for practical engineering requirements, such as process simulation. Thus, several efforts have been made to develop analytical equations of state suitable for confined fluids. The scope of this work consists of a modification to our previous modeling of fluid confinement in cylindrical pores based on cubic equations of state. By using new, more explicit mixing rules, a more consistent description of confined mixtures is obtained. Additionally, this modeling approach is extended to spherical pores. The proposed models displayed good predictive performance for the adsorption of binary and ternary mixtures, based on pure fluid adsorption data only, with an improvement relative to the previous modeling. It is shown that the adopted pore geometry can significantly affect the model performance.

1. Introduction

The thermodynamic properties of fluids confined in nanometric porous media can differ significantly from those of the bulk fluids, due to the inhomogeneity imposed by the geometric constraint and the interaction between fluid molecules and pore walls (molecule-wall interaction). The modeling of such properties is of practical importance to several applications, including gas and oil recovery from shale reservoirs. Thus, much work has been dedicated to studying the behavior of confined fluids (Peng and Yu, 2008; Vanzo et al., 2015; Tan and Piri, 2017). For instance, regarding the phase behavior, theoretical studies (Truskett et al., 2001; Zeng et al., 2010) and molecular simulations (Alvarez et al., 1999; De Grandis et al., 2007; Singh and Singh, 2011) indicate that a pure confined fluid may have a second critical point, related to a liquid-liquid transition. Regarding the adsorption phenomenon, Balbuena and Gubbins (1994) used density functional theory (DFT) to model a Lennard-Jones fluid and evaluate the effects of the interaction potential parameters and of the pore geometry (slit-like or cylindrical) on the adsorption amount and isosteric heat. These authors reported that the adopted confinement geometry plays an important role, especially for small pores, in which the fluid approaches a one-dimensional structure for cylindrical pores, or a two-dimensional structure for slit pores.

In an attempt to avoid computationally cumbersome modeling approaches, such as molecular simulations and DFT, several efforts have been made to develop analytical equations of state for confined fluids, which would be more suitable for process simulation.

* Corresponding author.
E-mail address: travalloni@eq.ufrj.br (L. Travalloni).

https://doi.org/10.1016/j.ces.2018.03.047
0009-2509/

List of symbols

a	energy parameter of the equation of state for bulk fluids
a_p	energy parameter modified by confinement
b	volume parameter of the equation of state for bulk fluids
b_p	volume parameter modified by confinement
E_{conf}	configurational energy
F_p	fraction of fluid molecules interacting with the pore walls
F_{pr}	value of F_p for random distribution of the fluid molecules
h	function of confinement in the expression of E_{conf}
k	Boltzmann constant
N	number of fluid molecules
N_{av}	Avogadro number
N_c	coordination number in a bulk fluid
NC	number of fluid components
P	pressure
q	internal partition function
Q	canonical partition function
R	ideal gas constant
r_p	pore radius
T	temperature
v	molar volume
V	total volume
V_f	free volume
V_p	pore volume
x	mole fraction

Greek letters

δ_p	molecule-wall interaction range
ε	intermolecular interaction energy
ε_p	molecule-wall interaction energy
θ	function of confinement in the expression of F_p
λ	de Broglie wavelength
μ	chemical potential
ρ	molecular density
σ	molecular diameter
ψ	attractive term of the equation of state for confined fluids

Subscripts

i, j	fluid component
max	maximum value (for molecular packing)

Superscripts

c	cylindrical confinement
PR	model based on the Peng-Robinson equation of state
s	spherical confinement
vdW	model based on the van der Waals equation of state

Many of the models proposed in the literature were obtained as extensions of usual models, such as the van der Waals equation of state (Schoen and Diestler, 1998; Zhu et al., 1999; Truskett et al., 2001; Giaya and Thompson, 2002; Zarragoicoechea and Kuz, 2002; Holovko and Dong, 2009; Travalloni et al., 2010; Kim et al., 2011; Dong et al., 2016), the Peng-Robinson equation of state (Travalloni et al., 2014; Barbosa et al., 2016), and SAFT (statistical associating fluid theory) equations of state (Martínez et al., 2007, 2017; Tan and Piri, 2015; Franco et al., 2017). In these publications, the confining pores are generally assumed to be slit-like or cylindrical. The different modeling approaches include the interfacial theory (Zhu et al., 1999), perturbation theory (Schoen and Diestler, 1998; Truskett et al., 2001; Giaya and Thompson, 2002; Martínez et al., 2007, 2017; Franco et al., 2017), scaled particle theory (Holovko and Dong, 2009), generalized van der Waals theory (Travalloni et al., 2010, 2014; Barbosa et al., 2016), and hybrid approaches (Tan and Piri, 2015; Dong et al., 2016), combining a bulk equation of state with the Young-Laplace equation. However, there is still room to further modeling efforts, with the aim of attaining an equation of state able to describe the complex behavior of confined fluids accurately.

In previous work (Travalloni et al., 2010), the van der Waals equation of state was extended to fluids confined in cylindrical pores, based on the generalized van der Waals theory and empirical expressions for some structural properties of the fluid. The obtained model relates the PVT variables with the pore radius and two additional parameters for each fluid, which are related to the molecule-wall interaction. The pure fluid model was successfully applied to the correlation of adsorption data. In addition, the extension of this model to fluid mixtures revealed its potential to predict the adsorption behavior of binary and ternary mixtures. The same methodology was used to extend the Peng-Robinson equation of state to confined fluids (Travalloni et al., 2014). However, the models proposed for confined mixtures in these publications were straightforward extensions of the models developed for pure fluids. In this way, despite the good performance when predicting mixture adsorption, the confined mixture modeling proved to be inconsistent with the ideal solution limit, as discussed in the next section. Nonetheless, our modeling of pure confined fluids (Travalloni et al., 2010, 2014) has no such drawback.

In this work, we start from our models for pure fluids confined in cylindrical pores, based on cubic equations of state (Travalloni et al., 2010, 2014), and propose a consistent way to extend them to confined mixtures, with more explicit mixing rules. We follow a similar approach for model development, using the empirical formulation of the confined fluid structural properties. Additionally, we extend this modeling to confinement in spherical pores, which are characteristic of certain materials, such as X- and Y-type zeolites (Auerbach et al., 2003). The predictive performance of the new models is evaluated against experimental mixture adsorption data, revisiting some of the adsorption systems considered in previous work in order to assess the effect of the new mixing rules. Also, the effect of the adopted pore geometry is evaluated and confined fluid models based on different equations of state for bulk fluids (van der Waals or Peng-Robinson) are compared.

2. Inconsistency in previous modeling of confined mixtures

In our previous work (Travalloni et al., 2010, 2014), conventional cubic equations of state were extended to fluids confined in cylindrical pores. First, models were developed for pure fluids. For example, the extension of the van der Waals equation to pure confined fluids was:

$$P = \frac{RT}{v - b_{pi}} - \frac{a_{pi}}{v^2} - \theta_i \frac{b_{pi}}{v^2}\left(1 - \frac{b_{pi}}{v}\right)^{\theta_i - 1} \times (1 - F_{pr,i})\left(RT\left(1 - \exp\left(-\frac{N_{av}\varepsilon_{pi}}{RT}\right)\right) - N_{av}\varepsilon_{pi}\right) \quad (1)$$

where P is the pressure, R is the ideal gas constant, T is the absolute temperature, v is the molar volume of the fluid, N_{av} is the Avogadro number, and the other variables (a_{pi}, b_{pi}, ε_{pi}, θ_i, and $F_{pr,i}$) depend on

the nature of fluid species i and of the confining pores. For confined mixtures, a straightforward extension of the pure fluid model was proposed:

$$P = \frac{RT}{v - b_p} - \frac{a_p}{v^2} - \sum_{i=1}^{NC}\left(x_i^2\theta_i\frac{b_{pi}}{v^2}\left(1 - \frac{x_i b_{pi}}{v}\right)^{\theta_i - 1}(1 - F_{pr,i})\right.$$
$$\left.\times\left(RT\left(1 - \exp\left(-\frac{N_{av}\varepsilon_{pi}}{RT}\right)\right) - N_{av}\varepsilon_{pi}\right)\right) \quad (2)$$

where NC is the number of fluid components, x_i is the mole fraction of component i, and a_p and b_p are parameters given by one-fluid mixing rules:

$$a_p = \sum_{i=1}^{NC}\sum_{j=1}^{NC}\left(x_i x_j\sqrt{a_i a_j}\left(1 - \frac{\sigma_i + \sigma_i}{5r_p}\right)\right) \quad (3)$$

$$b_p = \sum_{i=1}^{NC}(x_i b_{pi}) \quad (4)$$

where r_p is the pore radius, and a_i and σ_i depend on the nature of component i only. To find out if Eq. (2) satisfies the ideal solution limit, take two components (labeled as i and j) with identical properties, confined in the same pore. Hence, Eq. (2) becomes:

$$P = \frac{RT}{v - b_{pi}} - \frac{a_{pi}}{v^2} - \theta_i\frac{b_{pi}}{v^2}(1 - F_{pr,i})\left(RT\left(1 - \exp\left(-\frac{N_{av}\varepsilon_{pi}}{RT}\right)\right) - N_{av}\varepsilon_{pi}\right)$$
$$\times\left(x_i^2\left(1 - \frac{x_i b_{pi}}{v}\right)^{\theta_i - 1} + x_j^2\left(1 - \frac{x_j b_{pi}}{v}\right)^{\theta_i - 1}\right) \quad (5)$$

where a_{pi} is the pure component limit of a_p. The last term of Eq. (5) differs from that of Eq. (1), except for the pure fluid case. Therefore, for the same specification of pressure and temperature, the molar volume obtained for a binary mixture of identical components is different from that of the pure component. The same result applies to our previous models based on other equations of state (such as the Peng-Robinson equation), because all models share the last term. It follows that our previous modeling of confined mixtures is inconsistent with the ideal solution limit. However, this drawback does not affect our modeling of pure confined fluids, as well as its published results (Travalloni et al., 2010, 2014). In the next section, a new and consistent confined mixture modeling is provided.

3. Consistent equations of state and mixing rules

For pure fluids confined in cylindrical pores, the models proposed by Travalloni et al. (2010, 2014), based on well-known cubic equations of state, remain unchanged. Here, we present the new extensions of these models to confined mixtures, following the formulation of the van der Waals generalized theory (Sandler, 1985, 1990). For brevity, the main steps of model development are addressed, stressing the changes to the previous modeling of confined mixtures. For more details, the reader is referred to our previous work (Travalloni et al., 2010, 2014). Also, we highlight the parts of the formulation that are affected by the confinement geometry and propose their extensions to spherical pores.

The canonical partition function of a mixture is:

$$Q(T, V, N_1, \ldots N_{NC}) = \prod_{i=1}^{NC}\left(\frac{q_i^{N_i}}{\lambda_i^{3N_i}N_i!}\right)V_f^N\exp\left(\int_\infty^T\frac{E_{conf}}{kT^2}dT\right) \quad (6)$$

where V is the total volume, N is the number of molecules, q is the internal partition function of one molecule, λ is the de Broglie wavelength, V_f is the free volume, E_{conf} is the configurational energy, k is the Boltzmann constant, and subscript i refers to component i. For consistency with cubic equations of state and the one-fluid mixing rule for the volume parameter, the free volume is:

$$V_f = V - \sum_{i=1}^{NC}\left(\frac{N_i}{\rho_{max,i}}\right) \quad (7)$$

where $\rho_{max,i}$ is the molecular packing density of pure component i (a function of the pore geometry). The configurational energy expression was modified in this work to account for the confinement effects on the fluid mixture in an average way. From the pairwise additivity of the intermolecular interactions (first term) and of the molecule-wall interactions (second term), the configurational energy is:

$$E_{conf} = h\sum_{i=1}^{NC}\sum_{j=1}^{NC}\left(-\frac{N_j}{2}N_{c,ij}\sqrt{\varepsilon_i\varepsilon_j}\right) - NF_p\varepsilon_p \quad (8)$$

where $N_{c,ij}$ is the coordination number for the bulk fluid, which depends on the adopted equation of state (Travalloni et al., 2014), h is a factor that accounts for the mean reduction of the coordination number due to the spatial constraints imposed by the confinement (a function of the pore geometry), ε_i is the interaction energy between two molecules of component i, ε_p is the mean interaction energy between the fluid mixture and the pore wall, and F_p is the fraction of the mixture subject to this interaction. Previously, an empirical expression was proposed to model F_p for pure confined fluids (Travalloni et al., 2010). Here, the same expression is applied to confined mixtures, but using mean, composition-dependent parameters:

$$F_p = F_{pr} + (1 - F_{pr})\left(1 - \exp\left(-\frac{\varepsilon_p}{kT}\right)\right)\left(1 - \frac{\rho}{\rho_{max}}\right)^\theta \quad (9)$$

$$\theta = \frac{r_p}{\delta_p + \sigma/2} \quad (10)$$

where F_{pr} is the value of F_p for random distribution of the fluid molecules inside the pore (a function of the pore geometry), δ_p is the mean interaction range between the fluid mixture and the pore wall, σ is the mean molecular diameter of the mixture, ρ is the mean molecular density of the fluid, and ρ_{max} is the mean packing density of the mixture, given by the one-fluid mixing rule:

$$\frac{1}{\rho_{max}} = \sum_{i=1}^{NC}\left(\frac{x_i}{\rho_{max,i}}\right) \quad (11)$$

The other mean parameters of the confined mixture are obtained from linear mixing rules:

$$\sigma = \sum_{i=1}^{NC}(x_i\sigma_i) \quad (12)$$

$$\delta_p = \sum_{i=1}^{NC}(x_i\delta_{pi}) \quad (13)$$

$$\varepsilon_p = \sum_{i=1}^{NC}(x_i\varepsilon_{pi}) \quad (14)$$

where σ_i, δ_{pi}, and ε_{pi} are the molecular diameter, the molecule-wall interaction range, and the molecule-wall interaction energy for component i, respectively.

In this formulation, $\rho_{max,i}$, h, and F_{pr} are functions of the pore geometry and size. For F_{pr} (which appeared in Eq. (9)), an expression is obtained from the relation between the pore volume subject to the molecule-wall interaction and the pore volume available to the fluid molecules:

$$F_{pr} = \frac{(r_p - \sigma/2)^d - (r_p - \sigma/2 - \delta_p)^d}{(r_p - \sigma/2)^d} \quad (15)$$

where $d = 2$ for cylindrical pores and $d = 3$ for spherical pores. Eq. (15) was presented before for cylindrical pores (Travalloni et al., 2010) and its extension to spherical pores is straightforward; the only difference (d) results from the volume dependence on the radial dimension in each pore geometry.

For $\rho_{max,i}$ (which appeared in Eqs. (7) and (11)), an empirical expression was previously proposed for cylindrical geometry (Travalloni et al., 2010):

$$\rho_{max,i}\sigma_i^3 = c_1 - c_2 \exp\left(c_3\left(0.5 - \frac{r_p}{\sigma_i}\right)\right) + c_4 \exp\left(c_5\left(0.5 - \frac{r_p}{\sigma_i}\right)\right) \quad (16)$$

where c_k ($k = 1$–5) are universal parameters (Table 1). In this work, the same expression was fitted to available data for the packing of hard spheres in spherical containment with several r_p/σ_i ratios (Pfoertner, 2006). This fitting is shown in Fig. 1 and the parameters obtained for spherical geometry are shown in Table 1. Given the good fits to the available data in Fig. 1 and in the work of Travalloni et al. (2010), the same form of Eq. (16) is suitable for the packing density in both pore geometries, but with significant differences in some parameters. For consistency, the molecular diameter of each component is obtained from the bulk limit of Eq. (16) (c_1) and from the bulk volume parameter of the component, b_i (Travalloni et al., 2014):

$$\sigma_i = \sqrt[3]{c_1 \frac{b_i}{N_{av}}} \quad (17)$$

In this way, σ_i slightly depends on the adopted equation of state and pore geometry.

For h (which appeared in Eq. (8)), another empirical expression was previously proposed for cylindrical geometry (Travalloni et al., 2010) and adapted here to the new mixing rules:

$$h^c = 1 - \frac{2}{5}\frac{\sigma}{r_p} \quad (18)$$

where superscript c refers to the cylindrical geometry. On the other hand, for spherical geometry, the expression of h was based on the configurational data of hard spheres packed in spherical containment for several r_p/σ ratios (Pfoertner, 2006). From the coordinates of the individual spheres and assuming a range of 1.5 σ for the intermolecular interactions, the average coordination number in the packed structure ($N^s_{c,max}$) was obtained. Also, assuming that $N^s_{c,max} = 10$ for bulk fluids (i.e., for $r_p/\sigma \to \infty$), the following logistic-normal function was fitted to the relationship between $N^s_{c,max}$ and the pore size:

$$N^s_{c,max} = A + \frac{10 - A}{(1 + U\exp(-B(r_p/\sigma - M)))^{1/v}} - \frac{\exp(-(r_p/\sigma - \eta)^2/(2\varphi^2))}{\sqrt{2\pi}\varphi} \quad (19)$$

The fitting of Eq. (19) is shown in Fig. 2 and the universal parameters in this equation (A, U, B, M, v, η, and φ) are shown in Table 2. From this fitting, the reduction factor of the coordination number due to the spherical confinement was obtained:

$$h^s = \frac{N^s_{c,max}}{10} \quad (20)$$

where superscript s refers to the spherical geometry.

Given the partition function (Eq. (6)), all thermodynamic properties can be readily obtained, such as the pressure-explicit equation of state and the chemical potential of component i, which are given by:

$$P = kT\left(\frac{\partial(\ln Q)}{\partial V}\right)_{T,N_1,N_2,\ldots N_{NC}} \quad (21)$$

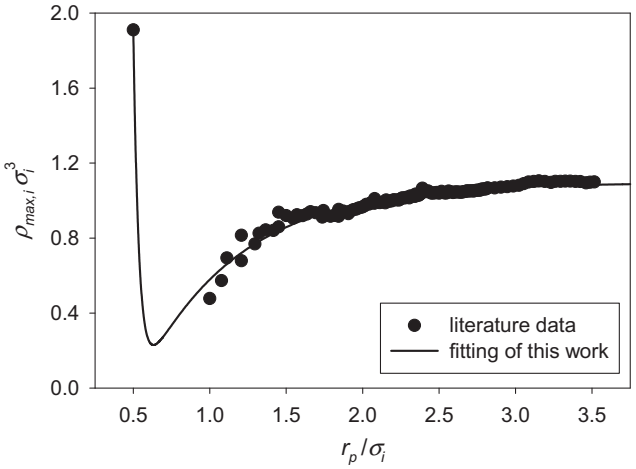

Fig. 1. Fitting of Eq. (16) to number density data (Pfoertner, 2006) for the packing of hard spheres in spherical geometry.

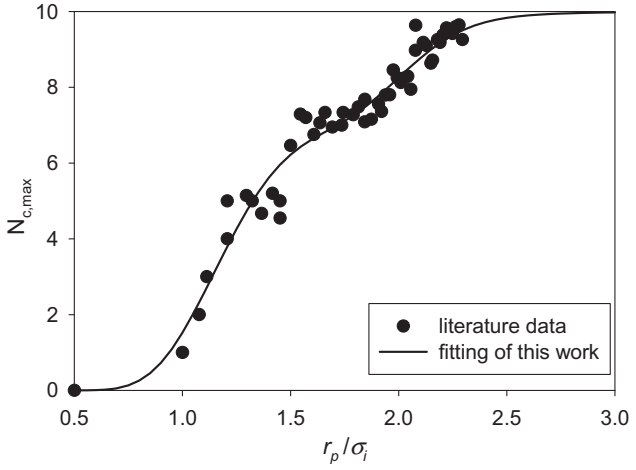

Fig. 2. Fitting of Eq. (19) to coordination number data (Pfoertner, 2006) for the packing of hard spheres in spherical geometry.

Table 1
Universal parameters of Equation (16).

Geometry	c_1	c_2	c_3	c_4	c_5
Cylindrical	1.158	0.479	0.621	0.595	4.014
Spherical	1.095	1.127	1.562	1.942	27.456

$$\mu_i = -kT\left(\frac{\partial(\ln Q)}{\partial N_i}\right)_{T,V,N_{j\neq i}} \tag{22}$$

Thus, the pressure-explicit equation of state for confined fluids is:

$$P = \frac{RT}{v-b_p} - \psi - \theta\frac{b_p}{v^2}\left(1-\frac{b_p}{v}\right)^{\theta-1}(1 - F_{pr})\left(RT\left(1-\exp\left(-\frac{N_{av}\varepsilon_p}{RT}\right)\right) - N_{av}\varepsilon_p\right) \tag{23}$$

where b_p is the confinement-modified volume parameter:

$$b_p = \sum_{i=1}^{NC}\left(x_i\frac{N_{av}}{\rho_{max,i}}\right) \tag{24}$$

and ψ is the confinement-modified attractive term of the model, which depends on the adopted equation of state:

$$\psi^{vdW} = \frac{a_p}{v^2} \tag{25}$$

$$\psi^{PR} = \frac{a_p(T)}{v(v+b_p)+b_p(v-b_p)} \tag{26}$$

where superscripts *vdW* and *PR* denote the van der Waals and the Peng-Robinson models, respectively, and a_p is the confinement-modified energy parameter, given by the one-fluid mixing rule:

$$a_p = h\sum_{i=1}^{NC}\sum_{j=1}^{NC}\left(x_i x_j\sqrt{a_i a_j}\right) \tag{27}$$

where a_i is the bulk energy parameter of pure component *i*. The obtained equation of state (Eqs. (23)–(26)) has the same form either for mixtures or for pure fluids, except for the model parameters, which depend on composition through one-fluid mixing rules (Eqs. (11)–(14), (24) and (27)). In this way, the proposed modeling satisfies the ideal solution limit, just as conventional equations of state do when they are coupled with one-fluid mixing rules. The chemical potential expression is more complex and is provided as FORTRAN calculation routines in the supplementary material.

Henceforth, the extension of the van der Waals equation of state to cylindrical confinement (Eqs. (23) and (25)) will be called vdW-C. Similarly, the extension of the Peng-Robinson model (Eqs. (23) and (26)) will be called PR-C for cylindrical confinement and PR-S for spherical confinement (according to the formulation of $\rho_{max,i}$, *h*, and F_{pr}).

4. Model evaluation methodology

The performance of the obtained models was evaluated in adsorption equilibrium calculations, as detailed elsewhere (Travalloni et al., 2010), for several adsorption systems, including systems addressed in previous work (Travalloni et al., 2010; Barbosa et al., 2016). The molecule-wall interaction parameters (ε_{pi} and δ_{pi}) were fitted to experimental data of pure fluid adsorption obtained from literature. Then, these estimated parameters were used to predict mixture adsorption behavior, without fitting binary interaction parameters. Following our previous methodology, the bulk parameters (a_i and b_i) were obtained from the critical temperature and volume of each pure fluid in the case of model vdW-C and from the critical temperature and pressure (and the acentric factor) in the case of models PR-C and PR-S.

5. Adsorption calculation results

5.1. Evaluation of the proposed mixing rules

The models for cylindrical confinement (vdW-C and PR-C) were used to evaluate the effect of the new mixing rules. Table 3 presents pore sizes and pore volumes (V_p) of different solid materials, molecular diameters of different pure fluids (consistent with the van der Waals or the Peng-Robinson equation of state), and molecule-wall interaction parameters estimated from pure fluid adsorption data (Nakahara et al., 1974; He and Seaton, 2003; Talu and Zwiebel, 1986). The properties of the MSC-5A and MCM-41 molecular sieves were reported by Nakahara et al. (1974) and He and Seaton (2003), respectively, or calculated from

Table 2
Universal parameters of Eq. (19) for spherical pores.

10^4A	*U*	*B*	*M*	10^4v	η	φ
−4.6849	0.2628	3.3445	−0.8141	3.2547	1.7938	0.2666

Table 3
Properties of different solids and fluids, and estimated parameters (ε_{pi}, δ_{pi}, and V_{p1} for mordenite) from literature experimental data of pure fluid adsorption for cylindrical pores.

Adsorbent	Adsorbate	Model vdW-C			Model PR-C		
		σ_i (nm)	ε_{pi}/k (K)	δ_{pi} (nm)	σ_i (nm)	ε_{pi}/k (K)	δ_{pi} (nm)
MSC-5A	Methane	0.40	1525[a]	0.353[a]	0.37	1543	0.294
r_p = 1.72 nm	Ethane	0.45	3110[a]	0.300[a]	0.43	3100	0.246
V_p = 0.56 cm^3/g							
MCM-41	Ethane	0.45	1259	0.328	0.43	1197	0.240
r_p = 1.35 nm	CO_2	0.39	1663	0.260	0.37	1411	0.199
V_p = 0.68 cm^3/g							
Mordenite	Propane	0.50	3399	0.033	0.48	3348	0.039
r_{p1} = 0.34 nm	CO_2	0.39	2716	0.005	0.37	2741	0.008
r_{p2} = 0.21 nm	H_2S	0.40	3799	0.003	0.37	3816	0.006
V_{p1}[b], V_{p2}[c]							

[a] Travalloni et al. (2010).
[b] 0.14 cm^3/g (vdW-C) or 0.12 cm^3/g (PR-C).
[c] 0.16 cm^3/g (vdW-C) or 0.14 cm^3/g (PR-C).

the measured properties with the assumption of a cylindrical pore geometry, which is a fair representation of the MCM-41 pores.

The properties of the mordenite zeolite were not reported by Talu and Zwiebel (1986) and standard crystal data were used instead (Myers, 1988). Hence, mordenite was assumed to be structurally heterogeneous, with two mean pore sizes: the largest one (r_{p1}) corresponding to 35% of the surface area, and the smallest one (r_{p2}) corresponding to 65% of the surface area. In view of the molecular diameters of propane, carbon dioxide, and hydrogen sulfide, the last two compounds could enter pores of both sizes. However, propane could only enter the largest pores, while the smallest ones would prevent the entrance of propane molecules. Thus, the propane adsorption data were only related to the largest pores, whose pore volume (V_{p1}) was estimated from these data, together with the molecule-wall interaction parameters of this compound. On the other hand, the total adsorbed amounts of CO_2 and H_2S had contributions from both pore sizes. The pore volume relative to the smallest pores (V_{p2}) was calculated from the surface area distribution between both pore sizes. The obtained V_{p1} and V_{p2} values (Table 3) are similar for models vdW-C and PR-C, which indicates that the confinement effect modeling is consistent. Given the V_{p1} and V_{p2} values, the molecule-wall interaction parameters of CO_2 and H_2S could be estimated from their adsorption data.

For the pure fluid adsorption data of Nakahara et al. (1974), a good fit was obtained with the vdW-C model (Travalloni et al., 2010) and the fit of the PR-C model was very similar (not shown). The fitting of both models to pure fluid adsorption data of He and Seaton (2003) and of Talu and Zwiebel (1986) is shown in Figs. 3 and 4, respectively. In Fig. 4, both models provided excellent fits

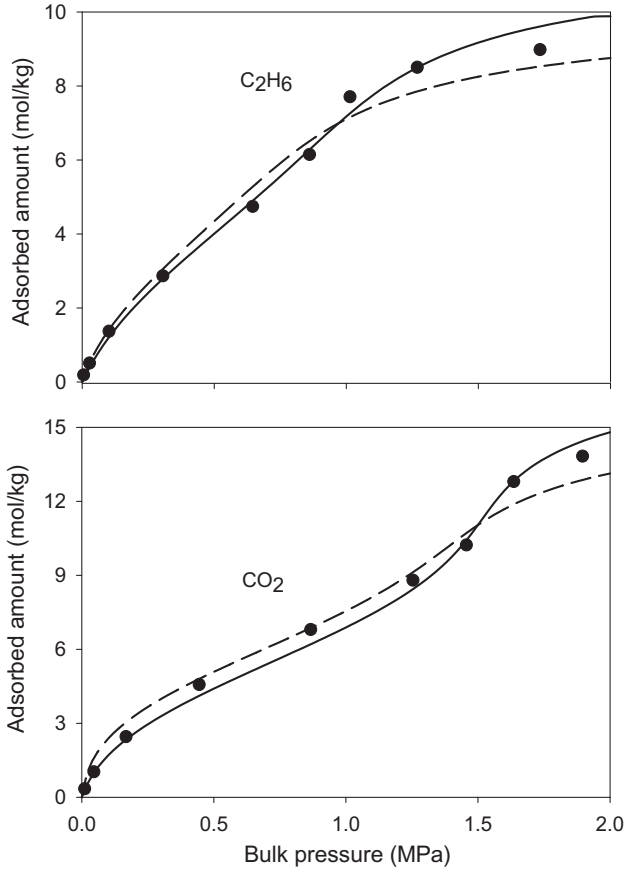

Fig. 3. Pure fluid adsorption on MCM-41 at 264.6 K. Symbols represent experimental data of He and Seaton (2003), dashed lines represent the fitting of model vdW-C, and full lines represent the fitting of model PR-C.

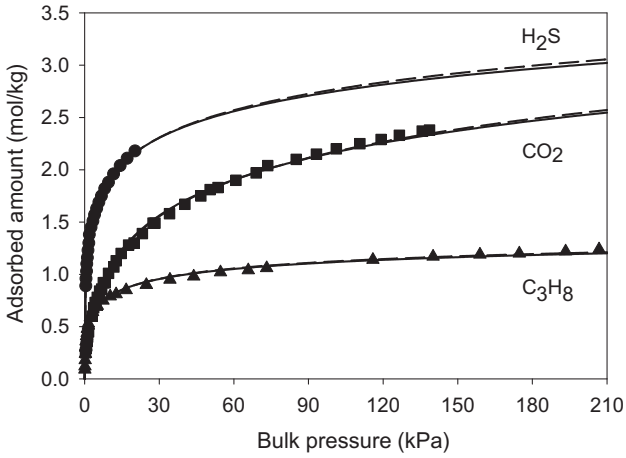

Fig. 4. Pure fluid adsorption on mordenite at 303.15 K. Symbols represent experimental data of Talu and Zwiebel (1986), dashed lines represent the fitting of model vdW-C, and full lines represent the fitting of model PR-C.

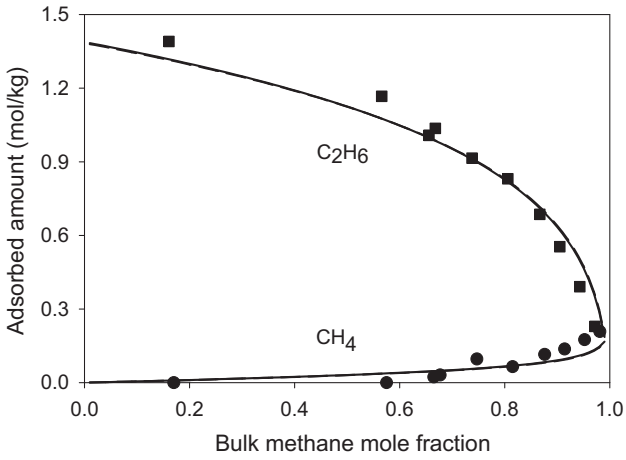

Fig. 5. Binary mixture adsorption on MSC-5A at 303.15 K. Bulk pressure is 13.3 kPa. Symbols represent experimental data of Nakahara et al. (1974), dashed lines represent the prediction of model vdW-C, and full lines represent the prediction of model PR-C.

for adsorption isotherms of type I in the IUPAC classification (Brunauer et al., 1940). In Fig. 3, both models also provided good correlations, but the isotherms are of type IV and this more complex profile was better correlated by the PR-C model, especially for CO_2.

Based on the parameters presented in Table 3, the predictive performance of models vdW-C and PR-C for mixtures was evaluated. Figs. 5 and 6 show experimental data of binary mixture adsorption on the MSC-5A molecular sieve (Nakahara et al., 1974) or on the MCM-41 molecular sieve (He and Seaton, 2003), together with the model predictions. In Figs. 5 and 6, the models provided very good predictions, which were similar in Fig. 5, while in Fig. 6 the PR-C model showed a better performance compared to the vdW-C model. Furthermore, upon comparing these results with those obtained from our previous modeling of confined mixtures (Travalloni et al., 2010; Barbosa et al., 2016), the new mixing rules significantly improved the prediction of methane adsorption on MSC-5A and of the mixture adsorption on MCM-41, especially with regards to CO_2.

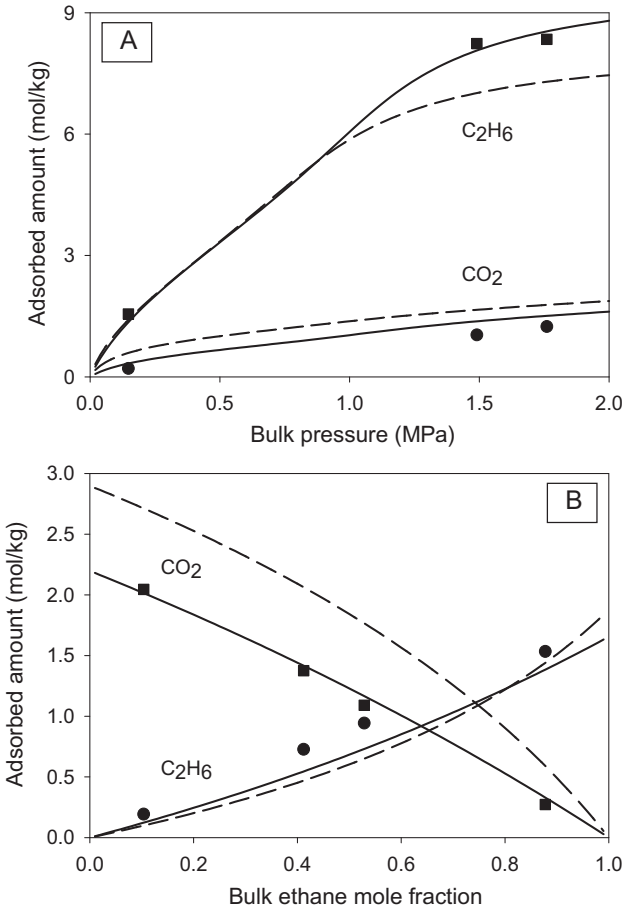

Fig. 6. Binary mixture adsorption on MCM-41 at 264.6 K. Bulk mole fraction of CO_2 is 0.1245 (A) and bulk pressure is 151.45 kPa (B). Symbols represent experimental data of He and Seaton (2003), dashed lines represent the prediction of model vdW-C, and full lines represent the prediction of model PR-C.

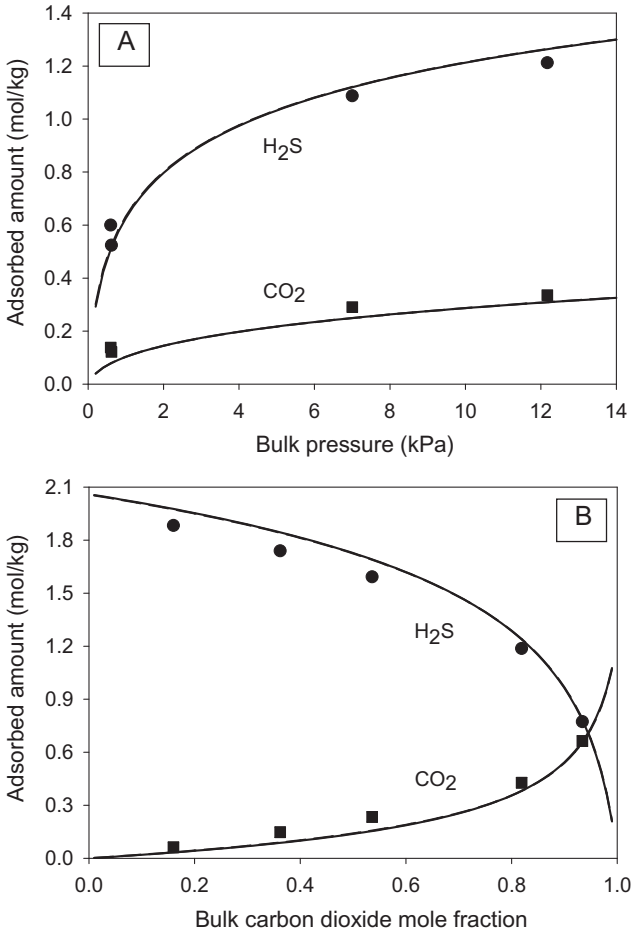

Fig. 7. Binary mixture adsorption on mordenite at 303.15 K. Bulk mole fraction of CO_2 is about 0.78 (A) and bulk pressure is about 15 kPa (B). Symbols represent experimental data of Talu and Zwiebel (1986), dashed lines represent the prediction of model vdW-C, and full lines represent the prediction of model PR-C.

Figs. 7–9 show experimental data of binary and ternary mixture adsorption on the mordenite zeolite (Talu and Zwiebel, 1986), together with the predictions of models vdW-C and PR-C. Again, very good predictions were obtained, which are quite similar for both models. It is noteworthy that the models accurately described the adsorption selectivity inversion for the mixture of propane and CO_2 (Fig. 8B) and provided a fair prediction of the ternary mixture adsorption (Fig. 9), based on pure fluid adsorption data only.

5.2. Effect of the confinement geometry on the model

In this section, the extensions of the Peng-Robinson equation of state for cylindrical and spherical confinements (PR-C and PR-S) were used to evaluate the effect of the confinement geometry on the modeling performance. Fig. 10 shows the same experimental data presented in Fig. 3 (He and Seaton, 2003), concerning pure fluid adsorption on MCM-41 molecular sieve, together with the fit of the PR-C model (the same as in Fig. 3) and of the PR-S model. This adsorbent has a remarkably homogeneous structure of long cylindrical pores with few interconnections, so that model PR-C should be more appropriate than PR-S in this case. For the fitting of model PR-S, the pore volume was the same as used with model PR-C (Table 3) and an equivalent size of spherical pores was calculated from the properties reported by He and Seaton (2003), namely, the specific surface area and the average cylindrical pore size. The equivalent spherical pore size and the estimated model parameters are shown in Table 4. While model PR-C correlated these adsorption isotherms very well, model PR-S was unable to accomplish this task due to the emergence of a spurious adsorbed phase transition. Moreover, Fig. 10 shows that the fitted PR-S model overestimated the maximum adsorbed amounts, suggesting that the pore volume should be lower than the one used in the modeling, which was based on reported textural properties of the adsorbent. As the conventional experimental methods for textural data evaluation can be unreliable for nanometric porous media (Landers et al., 2013), another fitting of model PR-S was attempted by estimating the pore volume together with the molecule-wall interaction parameters. However, an undue phase transition was still obtained in both adsorption isotherms (not shown), preventing a good fit of the PR-S model. This indicates that the pore geometry adopted in the modeling should be physically representative of the adsorbent structure, since model PR-C provided a good correlation of the adsorption on MCM-41 using the available textural data only.

Fig. 11 shows pure fluid adsorption data on 13X zeolite (Hyun and Danner, 1982), whose structure is mostly characterized by spherical cavities (Auerbach et al., 2003), together with the fittings of models PR-C and PR-S. In both fittings, the adopted pore volume was that reported by Hyun and Danner (1982), while the pore size was different in each case. For model PR-S, the standard size of the zeolite central cavity was used (Zhang et al., 2015). For model PR-C, an equivalent cylindrical pore size was calculated based on the

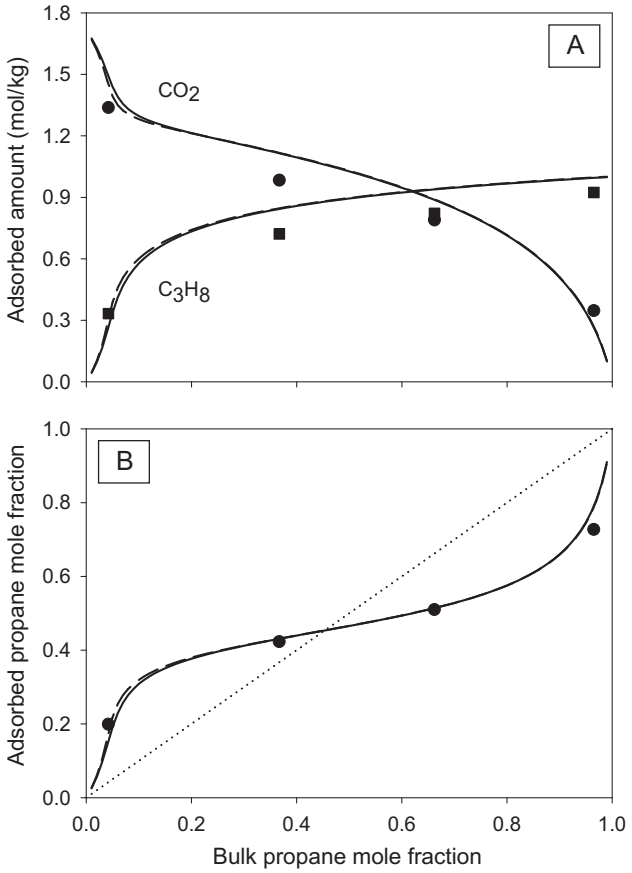

Fig. 8. Binary mixture adsorption on mordenite at 303.15 K. Bulk pressure is about 41 kPa. Symbols represent experimental data of Talu and Zwiebel (1986), dashed lines represent the prediction of model vdW-C, and full lines represent the prediction of model PR-C.

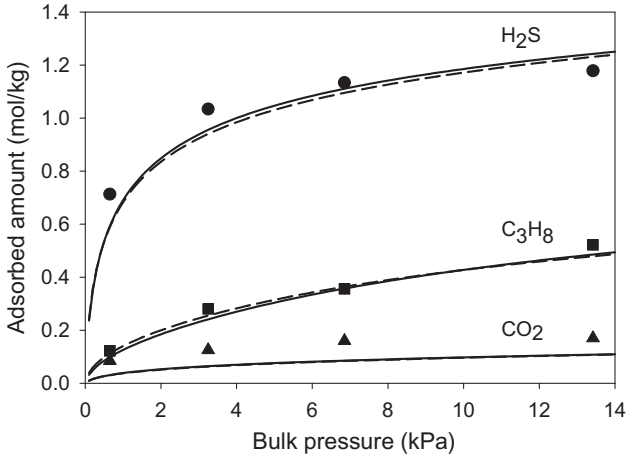

Fig. 9. Ternary mixture adsorption on mordenite at 303.15 K. Bulk mole fractions of propane and CO_2 are about 0.31 and 0.37, respectively. Symbols represent experimental data of Talu and Zwiebel (1986), dashed lines represent the prediction of model vdW-C, and full lines represent the prediction of model PR-C.

same surface area as for PR-S (i.e., the surface area resulting from the pore size and volume adopted for this model). The adsorbent properties and the estimated model parameters are shown in Table 4. Fig. 11 displays reasonable fits, with a slightly better performance of model PR-C (especially for ethylene). Less satisfactory

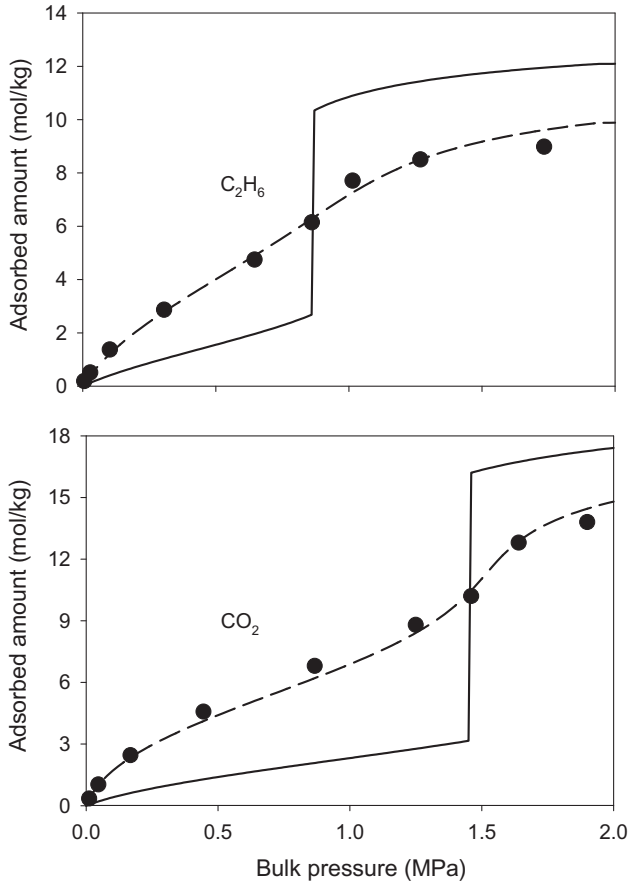

Fig. 10. Pure fluid adsorption on MCM-41 at 264.6 K. Symbols represent experimental data of He and Seaton (2003), dashed lines represent the fitting of model PR-C, and full lines represent the fitting of model PR-S.

fittings were obtained for isobutane, which deviates further from the spherical molecule assumption.

Fig. 12 shows experimental data of binary mixture adsorption on 13X zeolite (Hyun and Danner, 1982), together with the predictions of the PR-C and PR-S models (based on the parameters presented in Table 4). Both models qualitatively described the experimental data and accurately predicted the condition for adsorption selectivity inversion. However, model PR-C provided better results for ethylene-rich mixtures, possibly due to the better correlation of the pure fluid adsorption isotherms (Fig. 11). Therefore, although a better performance was expected for model PR-S in this case, the geometry inadequacy of model PR-C seems to have been compensated by the parameter fitting procedure.

6. Conclusions

In this work, our previous equation of state modeling of confined fluids was modified by the use of explicit, one-fluid mixing rules for the model parameters, resulting in a more consistent description of confined mixtures. The new modeling showed a good predictive performance for the adsorption of binary and ternary mixtures, based only on pure fluid fitting parameters, with an improvement relative to the previous modeling. Moreover, our modeling approach for cylindrical pores was extended to spherical pores. It was shown that the adopted pore geometry can affect the model performance significantly. Besides, comparing models based on different equations of state for bulk fluids (van der Waals or Peng-Robinson), most of the presented results were very similar, indicating that model performance is more influenced by the mod-

Table 4
Properties of different solids and fluids, and estimated parameters (ε_{pi} and δ_{pi}) from literature experimental data of pure fluid adsorption for different pore geometries.

Adsorbent	Adsorbate	Model PR-C				Model PR-S			
		r_p (nm)	σ_i (nm)	ε_{pi}/k (K)	δ_{pi} (nm)	r_p (nm)	σ_i (nm)	ε_{pi}/k (K)	δ_{pi} (nm)
MCM-41	Ethane	1.35	0.43	1197	0.240	2.02	0.42	907	0.169
V_p = 0.68 cm^3/g	CO_2		0.37	1411	0.199		0.36	938	0.129
13×	Ethylene	0.46	0.41	3398	0.189	0.68	0.40	3367	0.100
V_p = 0.30 cm^3/g	Isobutane		0.52	8727	0.097		0.51	6604	0.071

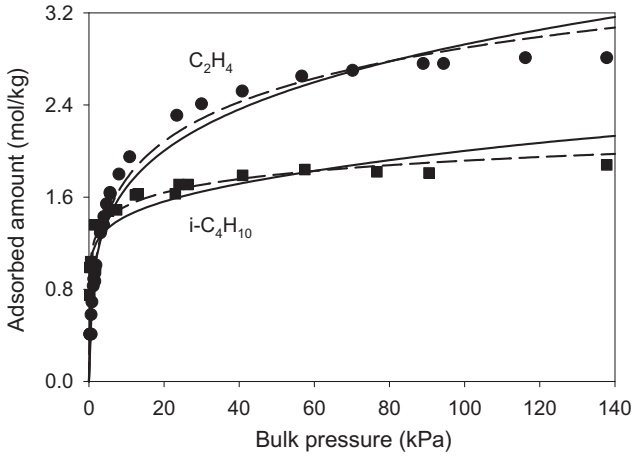

Fig. 11. Pure fluid adsorption on 13X at 298.15 K. Symbols represent experimental data of Hyun and Danner (1982), dashed lines represent the fitting of model PR-C, and full lines represent the fitting of model PR-S.

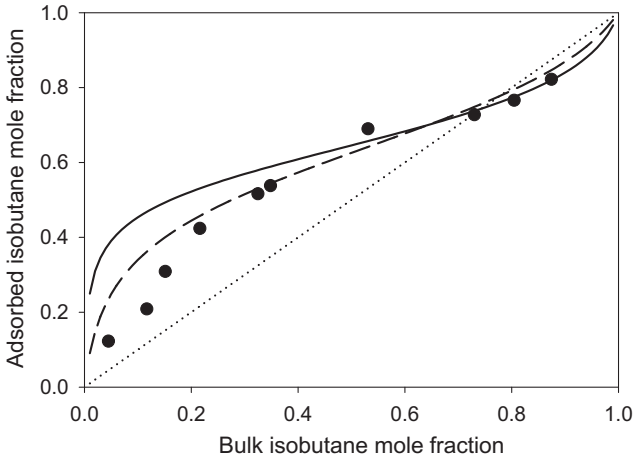

Fig. 12. Binary mixture (ethylene and isobutane) adsorption on 13X at 298.15 K. Bulk pressure is 137.8 kPa. Symbols represent experimental data of Hyun and Danner (1982), dashed lines represent the prediction of model PR-C, and full lines represent the prediction of model PR-S.

eling of confinement effects than by the modeling of intermolecular interactions in the fluid. However, the model based on the Peng-Robinson equation of state should be more appropriate for high pressure systems, such as gas and oil reservoirs.

Acknowledgments

We thank Ph.D. student Jacob L. Brown (Department of Chemical Engineering and Biotechnology, University of Cambridge) and Dr. Amaro G. Barreto Jr. (Escola de Química, Universidade Federal do Rio de Janeiro) for their questioning of our previous modeling of confined mixtures, for it helped us to find and correct the inconsistency mentioned in this work. Frederico W. Tavares and Gabriel D. Barbosa thank the financial support of CAPES, CNPq, and ANP. The participation of Marcelo Castier and Michelle L. D'Lima in this work was made possible by grants NPRP 8-1648-2-688 and NPRP 5-344-2-129, respectively, from the Qatar National Research Fund (a member of Qatar Foundation). The statements made herein are solely the responsibility of the authors.

Appendix A. Supplementary material

Supplementary data associated with this article can be found, in the online version, at https://doi.org/10.1016/j.ces.2018.03.047.

References

Alvarez, M., Levesque, D., Weis, J.J., 1999. Monte Carlo approach to the gas-liquid transition in porous materials. Phys. Rev. E 60, 5495–5504.
Auerbach, S.M., Carrado, K.A., Dutta, P.K., 2003. Handbook of Zeolite Science and Technology. Marcel Dekker, New York.
Balbuena, P.B., Gubbins, K.E., 1994. The effect of pore geometry on adsorption behavior. Stud. Surf. Sci. Catal. 87, 41–50.
Barbosa, G.D., Travalloni, L., Castier, M., Tavares, F.W., 2016. Extending an equation of state to confined fluids with basis on molecular simulations. Chem. Eng. Sci. 153, 212–220.
Brunauer, S., Deming, L.S., Deming, W.E., Teller, E., 1940. On a theory of the van der Waals adsorption of gases. J. Am. Chem. Soc. 62, 1723–1732.
De Grandis, V., Gallo, P., Rovere, M., 2007. The phase diagram of confined fluids. J. Molec. Liq. 134, 90–93.
Dong, X., Liu, H., Hou, J., Wu, K., Chen, Z., 2016. Phase equilibria of confined fluids in nanopores of tight and shale rocks considering the effect of capillary pressure and adsorption film. Indust. Eng. Chem. Res. 55, 798–811.
Franco, L.F.M., Economou, I.G., Castier, M., 2017. Statistical mechanical model for adsorption coupled with SAFT-VR Mie equation of state. Langmuir 33, 11291–11298.
Giaya, A., Thompson, R.W., 2002. Water confined in cylindrical micropores. J. Chem. Phys. 117, 3464–3475.
He, Y., Seaton, N.A., 2003. Experimental and computer simulation studies of the adsorption of ethane, carbon dioxide, and their binary mixtures in MCM-41. Langmuir 19, 10132–10138.
Holovko, M., Dong, W., 2009. A highly accurate and analytic equation of state for a hard sphere fluid in random porous media. J. Phys. Chem. B 113, 6360–6365.
Hyun, S.H., Danner, R.P., 1982. Equilibrium adsorption of ethane, ethylene, isobutane, carbon dioxide, and their binary mixtures on 13× molecular sieves. J. Chem. Eng. Data 27, 196–200.
Kim, H., Goddard III, W.A., Han, K.H., Kim, C., Lee, E.K., Talkner, P., Hänggi, P., 2011. Thermodynamics of d-dimensional hard sphere fluids confined to micropores. J. Chem. Phys. 134. 114502–1 11.
Landers, J., Gor, G.Y., Neimark, A.V., 2013. Density functional theory methods for characterization of porous materials. Coll. Surf. A 437, 3–32.
Martínez, A., Castro, M., McCabe, C., Gil-Villegas, A., 2007. Predicting adsorption isotherms using a two-dimensional statistical associating fluid theory. J. Chem. Phys. 126, 074707–074714.
Martínez, A., Trejos, V.M., Gil-Villegas, A., 2017. Predicting adsorption isotherms for methanol and water onto different surfaces using the SAFT-VR-2D approach and molecular simulation. Fluid Phase Equil. 449, 207–216.
Myers, A.L., 1988. Theories of adsorption in micropores. In: Rodrigues, A.E., LeVan, M.D., Tondeur, D. (Eds.), Adsorption: Science and Technology, 158. Kluwer Academic Publishers, Boston, pp. 15–36.
Nakahara, T., Hirata, M., Omori, T., 1974. Adsorption of hydrocarbons on carbon molecular sieve. J. Chem. Eng. Data 19, 310–313.
Peng, B., Yu, Y., 2008. A density functional theory for Lennard-Jones fluids in cylindrical pores and its applications to adsorption of nitrogen on MCM-41 materials. Langmuir 24, 12431–12439.
Pfoertner, H., 2006. Densest Packing of Spheres in a Sphere <http://www.randomwalk.de/sphere/insphr/ylspheresinsphr.html> (accessed July 22, 2006).

Sandler, S.I., 1985. The generalized van der Waals partition function – I: basic theory. Fluid Phase Equil. 19, 233–257.
Sandler, S.I., 1990. From molecular theory to thermodynamic models – part 1: pure fluids. Chem. Eng. Educ. 24, 12–19.
Schoen, M., Diestler, D.J., 1998. Analytical treatment of a simple fluid adsorbed in a slit-pore. J. Chem. Phys. 109, 5596–5606.
Singh, S.K., Singh, J.K., 2011. Effect of pore morphology on vapor-liquid phase transition and crossover behavior of critical properties from 3D to 2D. Fluid Phase Equil. 300, 182–187.
Talu, O., Zwiebel, I., 1986. Multicomponent adsorption equilibria of nonideal mixtures. AIChE J. 32, 1263–1276.
Tan, S.P., Piri, M., 2015. Equation-of-state modeling of confined-fluid phase equilibria in nanopores. Fluid Phase Equil. 393, 48–63.
Tan, S.P., Piri, M., 2017. Heat of capillary condensation in nanopores: new insights from the equation of state. Phys. Chem. Chem. Phys. 19, 5540–5549.
Travalloni, L., Castier, M., Tavares, F.W., Sandler, S.I., 2010. Thermodynamic modeling of confined fluids using an extension of the generalized van der Waals theory. Chem. Eng. Sci. 65, 3088–3099.
Travalloni, L., Castier, M., Tavares, F.W., 2014. Phase equilibrium of fluids confined in porous media from an extended Peng-Robinson equation of state. Fluid Phase Equil. 362, 335–341.
Truskett, T.M., Debenedetti, P.G., Torquato, S., 2001. Thermodynamic implications of confinement for a waterlike fluid. J. Chem. Phys. 114, 2401–2418.
Vanzo, D., Bratko, D., Luzar, A., 2015. Dynamic control of nanopore wetting in water and saline solutions under an electric field. J. Chem. Phys. B 119, 8890–8899.
Zarragoicoechea, G.J., Kuz, V.A., 2002. Van der Waals equation of state for a fluid in a nanopore. Phys. Rev. E 65. 021110–1 4.
Zeng, M., Jianguo, M., Zhong, C., 2010. Density functional theory integrated with renormalization group theory for criticality of nanoconfined fluids. J. Phys. Chem. B 114, 3894–3901.
Zhang, H.H., Wang, Y.M., Bai, P., Guo, X.H., 2015. Adsorption of acetic acid from dilute solution on zeolite 13X: isotherm, kinetic and thermodynamic studies. In: Xu, Q. (Ed.), Application of Materials Science and Environmental Materials. World Scientific, New Jersey, pp. 40–47.
Zhu, H.Y., Ni, L.A., Lu, G.Q., 1999. A pore-size-dependent equation of state for multilayer adsorption in cylindrical mesopores. Langmuir 15, 3632–3641.